10th International Conference on Contact Mechanics

CM2015, Colorado Springs, Colorado, USA

Numerical Analysis of Rolling Contact Fatigue Crack Initiation and Fatigue Life Prediction of the Railway Crossing

L. Xin[a], V.L. Markine[a], I.Y. Shevtsov[b]
aDelft University of Technology, Delft, The Netherlands
bProRail, Utrecht, The Netherlands

Abstract

The procedure for analysing rolling contact fatigue crack initiation and fatigue life prediction of the railway turnout crossing is developed. A three-dimensional finite element (FE) model is used to obtain stress and strain results, considering the dynamic effects of wheel-crossing rolling contact. Material model accounting for elastic- plastic isotropic and kinematic hardening effects is adopted. The results from FE analysis are combined with J-S fatigue model that is based on critical plane approach, and fatigue crack initiation life is predicted according to different positions on the crossing. The most critical position on the crossing is found and number of cycles to crack initiation is predicted.

1. Introduction

Turnouts are important elements in the railway infrastructure as they provide guidance to the traffic. It consists of a switch panel, a closure panel and a crossing panel. Because of the geometrical discontinuities in the crossing panel, high impact forces are generated here. Moreover, since the crossing profiles are gradually changed to the normal rail, the small width and radius of the crossing nose make it the weakest point in the crossing structure. Therefore, high impact forces and crossing geometry together result in severe damage in the crossing.

In the Netherlands, rolling contact fatigue (RCF) is a severe problem that causes most of the operation disturbance of the turnout. There are around 400 crossings replaced per year and two crossings per week are urgently to be repaired. The replacement budget reaches 6.4 million per year. Obviously, solutions for the RCF related problems are urgently needed. Figure 1 shows the typical defects in the turnout. It is found that the damage in the crossing nose is dominated by shelling which is rarely found in the normal line. Generally, shelling is a subsurface defect that occurs at the gauge corner of the high rail in curves of railways with a high axle load and can crack at any level [1]. In the crossing, because of the high impact it is more likely to form such kind of damage (Figure 1b). According to the field observations, the crossing nose experiences large plastic deformation caused by the impact and the subsurface cracks may occur, which becomes shelling at a later stage. Besides shelling, vertical cracks are also observed in the crossing nose (Figure 1c).

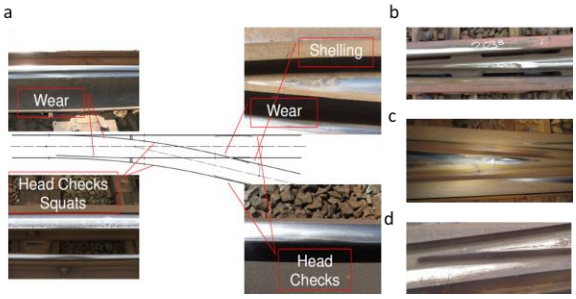

Fig. 1. Damage in the turnout.

The high impact forces in the crossing nose can accelerate the formation of damage and magnify the imperfection of the local/global geometry or material. For example, geometrical error of the wing rail can bring the impact position on the crossing nose much earlier, which results in damage of the nose. Other causes might be the inclusions in the material itself, which form the cracks underneath the surface. Welding process may also result in the later damage of the crossing. However, some causes of the damage in the crossing are still not known yet. Other defects

such as head checks and squats at the rear of the crossing, wear and cracks in the wing rails (Figure 1d) are also the typical damage defects in the crossing which require welding/grinding or replacement of the crossing.

Recently, several studies on damage of the turnout crossing have been conducted. In [2] the dynamic forces in a turnout crossing were analysed using the two-dimensional (2D) finite element (FE) model. By optimising the track stiffness for a given rail geometry, the dynamic forces were reduced. A three-dimensional (3D) dynamic model of the crossing and a quasi-static submodel were developed in [3] to investigate crossing damage, by choosing the stress triaxiality as the damage initiation factor. The cyclic deformation of a crossing nose was taken into account and two materials were compared in [4]. In [5] damage was assumed to be quadratically proportional to the impact force. The objective function was then formulated with the intension to distribute the impact damage uniformly throughout the transition zone. The influence of a stochastic spread in traffic parameters on damage in the S&C was assessed in [6]. In [7] the index FI_{surf} based on the contact forces was used to identify the surface initiated rolling contact fatigue (RCF) defects of the turnout. Multi-scale FE approach was used to study the RCF of three crossing nose materials [8], in which the crack development and growth of the three materials were obtained and compared.

However, these studies did not take the different stress types and stress directions into account to predict fatigue life of the rail. Also, because of the variable crossing geometry, damage in different locations should be considered separately. In this paper, stress and strain distributions at the different positions on the crossing are considered. Jiang and Sehitoglu fatigue model for determining the fatigue life of the crossing are included. Numerical simulations are conducted to identify the most possible area of damage in the crossing and predict possible fatigue crack initiation.

2. Fatigue life analysis

For fatigue life analysis various approaches have been proposed to estimate the mean stress effect, including stress-life models used at high cycle fatigue (HCF), strain-life models for low-cycle fatigue (LCF) and stress/strain-life models, which used a strain energy quantity for both HCF and LCF. For this model Smith et al. advocated that the product of $\sigma_{max}\varepsilon_a$ (SWT parameter, the maximum tensile stress, σ_{max} and the total strain amplitude, ε_a) controls the fatigue life. However, for cyclic loads that involve relatively large compressive mean stress, the stress/strain-life models might be non-conservative.

Moreover, regarding to the SWT parameter, tests of a 304 sainless steel under both proportional and non-proportional loading were conducted in [10]. It concludes that the contributions of shear components to damage on the maximum principal strain range plane are more and more significant by increasing the non-proportional degree. However, in the SWT parameter only the normal components are considered [11]. Therefore, several modifications of the SWT parameter have been proposed, which are summarized in [9].

It is known that in wheel/rail rolling contact problem the rails are subjected to multi-axial and non-proportional loadings. Therefore, in this paper a combined energy-density based and critical plane approach for low cycle fatigue problem proposed by Jiang and Sehitoglu is used to predict the fatigue life of the crossing. This approach is strongly dependent on the stress state, loading histories and material type. In this criterion, it considers that both normal and shear components of stress and strain on the critical plane contribute to the damage of the material [12]. The damage/fatigue parameter FP is defined as:

$$FP = \langle \sigma_{max} \rangle \frac{\Delta\varepsilon}{2} + J\Delta\gamma\Delta\tau \qquad (1)$$

Where $\langle\ \rangle$ is the MacCauley bracket, $\langle x \rangle = 0.5(|x| + x)$; σ_{max} is the maximum normal stress; $\Delta\varepsilon$ is the normal strain range; $\Delta\gamma$ is the shear strain range; $\Delta\tau$ is the shear strain range. These quantities are on the critical plane which is defined as the plane with maximum FP. Through a tensor rotation for the stress and strain, the maximum FP and the critical plane are determined by surveying all the possible planes at a material point. The energy-density should be computed as the damage parameter on every material plane and for every increment of loading.

Here FP is expressed in products of the stress and strain range components, as $\alpha\Delta\sigma\Delta\varepsilon + \beta\Delta\tau\Delta\gamma$, where the influence of each product is weighted by the material and load dependent constants, α and β. The model is physically associated with two loading modes for fatigue initiation and fracture: tension is represented by $\alpha\Delta\sigma\Delta\varepsilon$ and shear by $\beta\Delta\tau\Delta\gamma$. It

should be noted that cracking behaviour is material and loading magnitude dependent. Some material display shear cracking, some exhibits tensile cracking and some displays a mixed cracking behaviour. It was concluded that a material tends to display shear cracking in low cycle fatigue but tensile or mixed cracking at high cycle fatigue lives [13].

The fatigue life to initiation, N_f, is computed on this crack plane as [14,15]:

$$FP_{max} = \begin{cases} (\langle\sigma^{max}\rangle\frac{\Delta\varepsilon}{2} + J\Delta\tau\Delta\gamma)_{max} = \frac{(\sigma_f')^2}{E}(2N_f)^{2b} + \sigma_f'\varepsilon_f'(2N_f)^{b+c} \\ (\langle\sigma^{max}\rangle\frac{\Delta\varepsilon}{2} + J\Delta\tau\Delta\gamma)_{max} = \frac{(\tau_f')^2}{E}(2N_f)^{2b} + \tau_f'\gamma_f'(2N_f)^{b+c} \end{cases} \quad (2)$$

Where E, G are the elastic/shear modulus; σ_f', τ_f' are the tensile/shear fatigue strength coefficients; $\varepsilon_f', \gamma_f'$ are the tensile/shear fatigue ductility coefficients. The material constants are obtained from [11,17]. The composition of FP should be analysed to determine which form of the formula should be used for fitting shear or tensile cracking.

The combined energy density based and critical plane models have been shown to commendably adapt to experimental data, with respect to both fatigue life and crack plane orientation. This is essential for the RCF problems where the non-proportional loading produces additional hardening in the material, in contrast to proportional loading [15]. There are some other applications of this model. For example, the effects of different rail cant, superelevation, coefficients of friction and radius were investigated in [14], which also stated that if the shear stress/strain was dominant, the shear form of the formula should be adopted. The stress-strain history and the crack iniation lives of bainitic and pearlitic rail steels were determined under rolling contact loading by implementing the semi-analytical J-S model [16]. In [17] the head check initiation life prediction of rails was conducted considering critical plane approach, and the predictions were compared with data in the field.

3. Material model

Generally speaking the material response to cyclic loading can be classified as four categories: elastic, elastic shakedown, plastic shakedown and ratcheting [18]. A material subjected to repeated rolling contact loading undergoes multiaxial and non-proportional strain cycling. Under such kind of loading the rail material could fail by low cycle fatigue or by accumulation of a directional plastic strain. This latter failure is called ratchetting failure and occurs in rolling/sliding contacts with evidence of excessive plastic flow near the surface. It is revealed also in the crossing by the excessive deformation and metal flow measured after heavy axle load traffic[9].

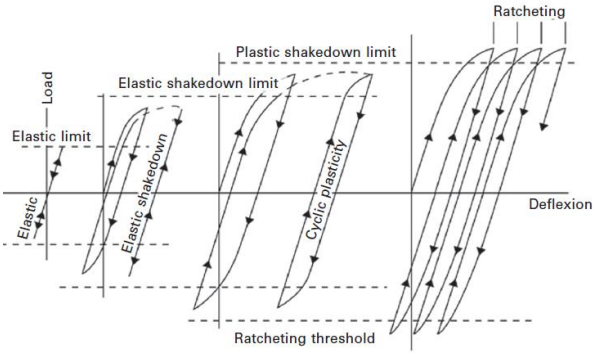

Fig. 2. Material response to cyclic loading [18]

Since the crossing is under the heavy repeated impact load, plastic deformation is generated and accumulated. Therefore, the crossing is modelled with an elastic-plastic isotropic and kinematic hardening material model. It is based on Lemaitre and Chaboche [1990] material model and is available in LS-DYNA [19]. It is suited to model nonlinear isotropic and kinematic plasticity and accounts for cyclic hardening and ratcheting. The size of the surface increase as function of the equivalent plastic strain, ε^p:

$$\sigma_y = \sigma_{y0} + H\varepsilon^p \quad (3)$$

Where σ_{y0} is the initial stress; H is the isotropic hardening modulus.

The rate of evolution of the kinematic component is a function of the plastic strain rate:

$$\dot{\alpha} = [Cn - \gamma\alpha]\dot{\varepsilon}^p \quad (4)$$

Where, α is the back stress, and n is the flow direction. C and γ are the parameters for the back stress. The term, $\gamma\alpha\dot{\varepsilon}^p$, introduce the nonlinearity into the evolution law. The parameters of the material model can be found in [20]. The material parameters for elastic behaviour, isotropic hardening H and kinematic hardening C and γ are listed in Table 1.

Table 1. Material properties.

Parameters (unit)	Value	Parameters (unit)		Value
Initial yield stress, σ_{y0} ,	500	Young's Modulus	Railpad	2.40e+8

(MPa)		(Pa)		
Isotropic plastic hardening modulus, H, (Gpa)	20		Sleeper	3.00E+10
Kinematic hardening modulus, C, (Gpa)	13.2		Ballast	1.34E+8
Kinematic hardening parameter, γ	3.12	Poisson's ratio	Railpad	0.47
Young's modulus (GPa)	200		Sleeper	0.18
Poisson's ratio	0.30		Ballast	0.20
Mass (kg/m^3)	7850			
Tensile fatigue strength , σ_f' (MPa)	936	Tensile fatigue ductility coefficients, ε_f'		0.103
Shear fatigue strength coefficients, τ_f' (MPa)	468	Shear fatigue ductility coefficients, γ_f'		0.1545
b	-0.089	c		-0.559

4 Numerical modeling

4.1 FE modeling of the wheel/crossing impact

In this paper, a three dimensional (3-D) explicit finite element model (Figure 3a) with the implementation of elastic-plastic nonlinear kinematic hardening material is developed to simulate the dynamic response of a whole wheelset while it is passing a crossing [21, 22]. The model consists of a crossing section of 4540mm long and the S1002 unworn wheel profile is used. The turnout modelled here is the curved one with the radius of 725m and the crossing angle of 1:15. The crossing nose in the model is built using four main cross-sections as they are defined in the drawings from the manufacturer (Figure 3b). These four cross-sections are located on the distances of 10a (mm), 10a (mm) and 50a (mm) from each other, where the 'a' is equal to the crossing angle of the turnout (e.g. for 1:15 turnout a=15). All the components in the model including railpads, sleepers and ballast are modelled using solid elements, which enables performing the stress and strain analysis. Fine mesh is used in the contact regions, i.e. the crossing nose, railhead and wheel tread (Figure 3c).

In the beginning of each simulation the wheelset is placed on the wing and stock rail in the middle of the track without any lateral displacement or rotation, so that no angle of attack and no lateral displacement are applied. The wheelset has no constraints in any degree of freedom. The wheelset travels in the facing through route. During rolling the wheelset has the lateral displacement and angle of attack as a result of the geometrical discontinuities in the crossing. The axle load of 150kN is applied to the wheelset. The wheelset moves along the crossing with the translational velocity of 130 km/h and the angular velocity of 78.5 rad/s. Initially (during the stabilisation phase), the wheels come in contact with the rails due to application of the gravity force and the axle load. In order to minimize the initial system vibration, the preload procedure was used. During the simulation (after the stabilisation phase), the wheelset rolls over the crossing and the wheel/crossing contact behaviour on the local scale is studied. The model has been validated by field measurements in [22], which shows the ability to capture the wheel/crossing impact.

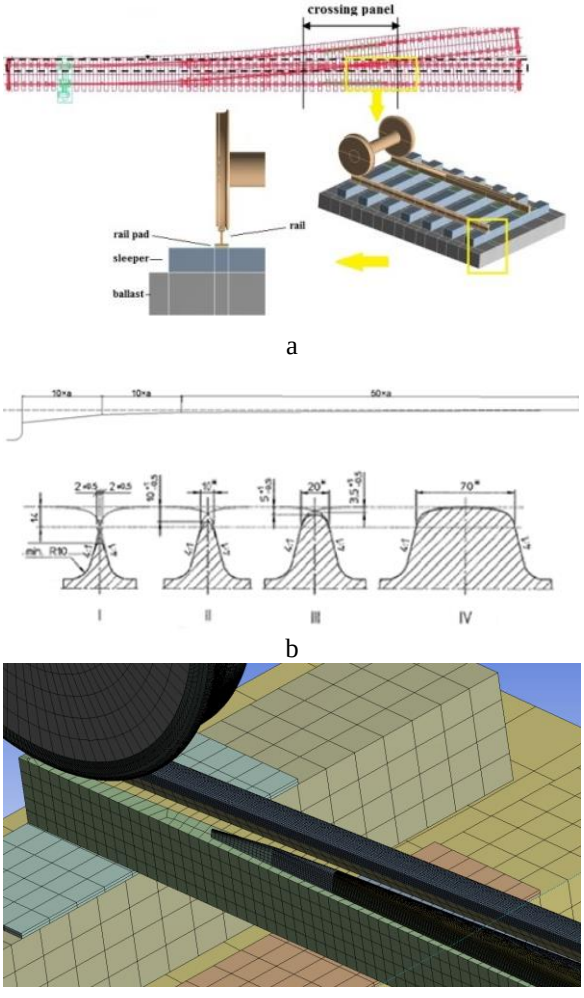

a

b

c

Fig. 3. (a) schematic of the finite element model, (b) drawing from the manufacturer (c) mesh of the wheel, crossing and the substructures.

4.2 Analysis procedure

The dynamic responses such as contact forces between the wheel and the crossing, crossing nose displacements and accelerations, stresses in rail material as well as in sleepers and ballast can be obtained using the model presented in the previous Section. The stress and strain in the crossing will be analysed in details. The procedure of the fatigue life analysis is as follows. Firstly, the stress/strain state of the whole crossing (1050mm) is analysed. The Von Mises stress is chosen as the criteria to determine the most critical wheel position (P_{cr}) on the crossing where damage can occur. Then the stress/strain state in this position is analysed. Pressure, surface shear stress as well as plastic deformation are chosen to describe the contact conditions.

In the selected critical wheel position (P_{cr}), the element with the maximum Von Mises stress value is selected for the fatigue parameter (FP) calculation (Section 2). The FP value for each plane in this element is calculated according to (1) and the plane with the maximum FP value is treated as the critical plane where the fatigue crack is most probably can be initiated. The number of cycles to the fatigue crack initiation (N_f) is obtained for this plane, which is also the minimum N_f for this critical point in critical location P_{cr}.

Finally, the angle of the critical plane and the corresponding N_f are calculated as described above for the whole crossing in five selected positions (P_{cr1}, P_{cr2} to P_{cr5}). N_f is then compared within these positions and the most critical position is obtained.

5. Numerical Results and fatigue analysis

5.1 Stress and strain response

Since the geometry varies along the crossing, contact conditions such stress and strain also change at different positions. Figure 4 shows an example of the Von Mises stress state at the different wheel-rail contact positions on the crossing. From this figure it can be seen that the contact angle, contact point as well as the contact radius change along with the different (longitudinal) contact positions. For example, when the wheel/crossing contact is in the front part of the crossing (Figure 4a), the rail radius is small and the contact patch is therefore narrower as compared to the contact at the rare part of the crossing (Figure4d).

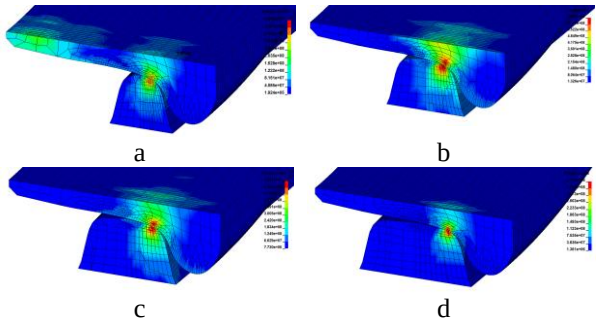

Fig. 4. Von-Mises stress distribution at different positions on the crossing.

The Von Mises stress distributions on the wing rail and the whole crossing are plotted in Figure 5a. The horizontal axis represents the distance from the nose point. The total length of the crossing is 1050mm (1:15 crossing) and after 1050mm the height of crossing nose turns to be the same as the normal rail, which is therefore not considered here. Before the inner wheel comes in contact with the crossing, it is only supported by the wing rail, later the wheel has contact with both wing rail and crossing. The wheel/crossing contact starts at a position of 334mm from the nose point. The maximum Von Mises stress with a value of 707MPa occurs at P= 502mm on the crossing.

Regarding to plastic strain, it could be seen that in the simulation most of the plastic strain occurs in the area of 500mm-760mm. The maximum effective plastic strain of 8.79e-3 occurs at P=507mm. Comparing with the field observation of a crossings 1:15 [23.], it correlates well. Figure 5b shows that large plastic deformation occurs in the area (red circle) of 500mm-800mm in the field.

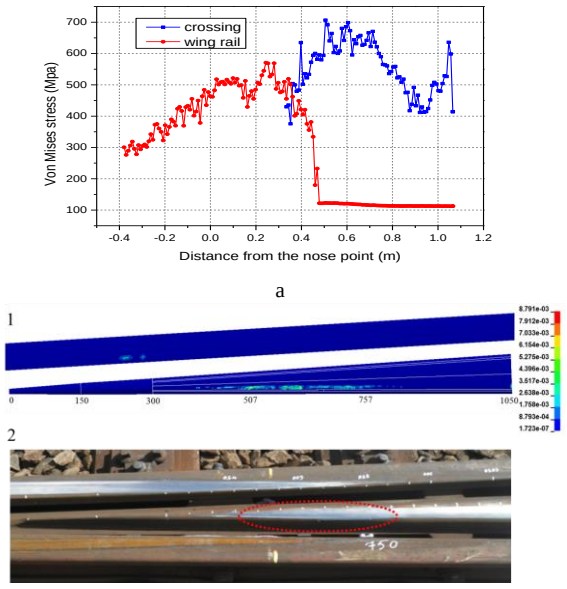

b

Fig. 5. (a) Von Mises stress distribution of the crossing, (b) plastic strain from the simulation and plastic deformation from the field.

As mentioned before, the position with the maximum Von Mises stress is treated as the critical position (P_{cr}) for crack initiation. The stress state is then evaluated for this position. Von Mises stress, contact pressure and surface shear stress are shown in Figure 6. Figure 6a plots the highest Von Mises stress in the middle. Figure 6b shows that the maximum contact pressure has a value of 1375MPa. By Hertz contact theory the maximum contact pressure in this case is 2680MPa. Both values are comparable to [24], in which Hertz contact theory and elastic-plastic FE method were used for contact pressure calculation of a turnout crossing. For interface shear stress it is stated in [22] that it is strongly influenced by friction coefficient, however in this paper only one friction coefficient is considered.

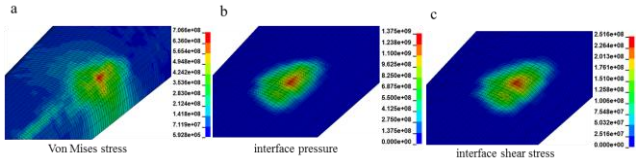

Fig. 6. Stress plots of the critical position.

5.2 Fatigue life calculation of a critical material point

The stress distributions of P_{cr}, including maximum shear stress, the 1st, 2nd and 3rd principal stresses are shown in Figure 7. It could be seen from the three principal stresses that most of the area in crossing is subjected to compressive stress, which is due to the high impact force on the crossing. According to Mohr's circle for three-dimensional stress state, it is known that if three principal stresses of a certain point in the crossing are all compressive, the normal stresses of all planes are compressive. In these points (mainly on the top) shear cracking dominates and governs the fatigue life. The term $\langle\sigma_{max}\rangle\frac{\Delta\varepsilon}{2}+J\Delta\gamma\Delta\tau$ in the fatigue parameter (1) is then reduced to $J\Delta\gamma\Delta\tau$. Also, in this case the number of cycles before crack initiation N_f should be calculated in the form of shear components (2). Regarding to the points which have both tensile and compressive stresses, tensile and shear cracking should be both considered.

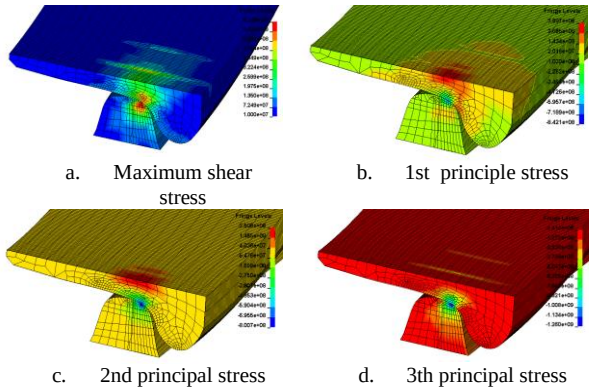

a. Maximum shear stress
b. 1st principle stress
c. 2nd principal stress
d. 3th principal stress

Fig. 7. Stress distributions at P_{cr}.

Therefore for fatigue analysis at P_{cr}, several points in both compressive area and tensile/compressive area are selected for comparison. The stress and strain components of the selected points are plotted in Figure 8.

First of all, the critical point, which has the maximum Von Mises stress value is selected. It locates at the rail surface, with compressive stresses in all planes. The vertical distance from rail surface is therefore plotted as 0mm in horizontal axial in Figure 8. Besides, four other points beneath the critical point are also selected for the fatigue life analysis. The vertical distances from the rail surface to these four points are 1.316mm, 2.606mm, 3.994mm and 7.006mm respectively. From Figure 8 it could be seen that as the vertical distance increases, the stress and strain components, especially in the vertical direction decrease significantly. These components further determine the FP value in these points.

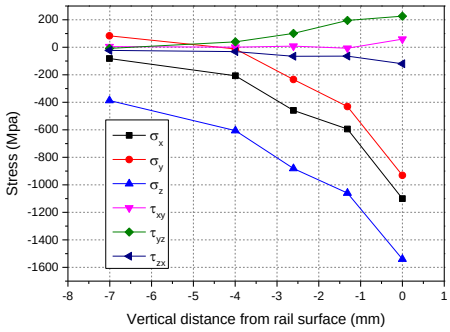

a

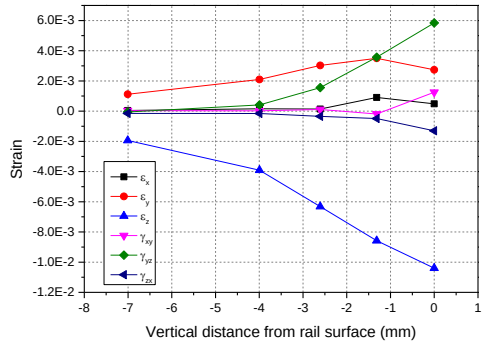

b

Fig. 8. stress (a) and strain (b) components of the elements at different vertical positions.

By the tensor rotation transformation the FP value for any plane of the critical point can be calculated. The plane with the maximum FP value is treated as the critical plane. At this plane two angles θ and φ are obtained (see Figure 9a) which represent the spherical angles of the normal vector $\vec{n}$ of the critical plane/crack initiation plane to the coordinates system attached to the railhead surface. The angle θ represents the angle between the normal vector and the longitudinal (rolling) direction. It could be seen from Figure 9a that the angles θ in different vertical positions have good correlation with each other, which are in the range from 85° to 100°. The critical point has the angle of 87.2°. However, the angles φ, which represent the angle between the normal vector and the vertical direction, differ a lot. The reason might be that the loading conditions on the subsurface points are different from the surface node, so that the angle to the vertical direction varies.

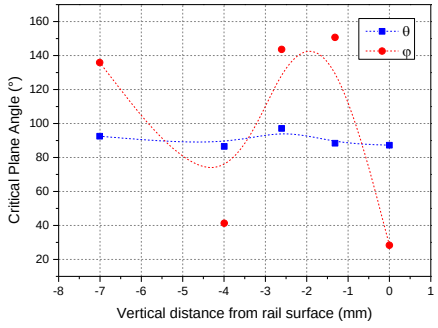

a

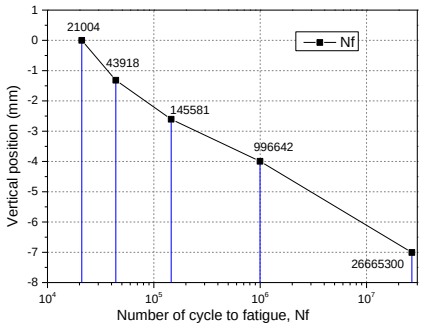

b

Fig. 9. (a) angles of the critical planes, (b) number of cycles to fatigue.

The number of cycles to fatigue crack initiation N_f is calculated and plotted in Figure 9b. As mentioned above, the tensile or shear forms of the N_f equations are considered separately for different stress state. From Figure 9 it can be seen that as the vertical distance from the rail surface increases, the fatigue life increase greatly. The fatigue life to crack initiation is therefore determined by the critical point with N_f=21004 cycles.

5.3 Fatigue life calculation of the whole crossing

Due to the geometrical variation of the crossing, contact conditions including contact angle and size of contact patch etc. vary a lot along the whole crossing, which has been shown in Figure 4. Therefore stress/strain analysis as well as the fatigue life analysis at different positions are necessary. The critical points of five contact positions (P_{cr1}, P_{cr2} to P_{cr5}) on the crossing are selected. The angles of the critical planes as well as the contact positions (coordinates) and N_f are plotted in Figure 10a and 10b respectively. Regarding to the angle of the critical plane/crack initiation plane, similar results are shown that the angle θ correlates well (85° to 95°), however angle φ varies greatly. It may lead to the deduction that for crack initiation plane, in this case the angle between this plane to longitudinal direction has a possible angle of 85° to 95°, while the angle between this plane to vertical direction is difficult to predict.

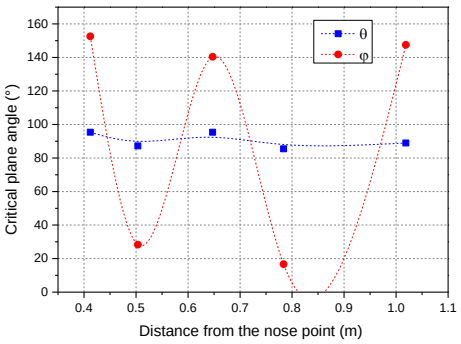

a

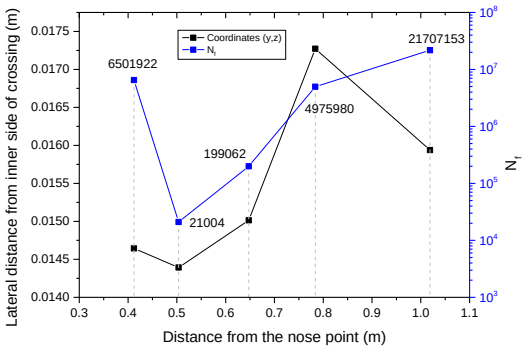

b

Fig. 10. (a) angles of the critical planes, (b) number of cycles to fatigue.

Figure 10b presents the lateral and longitudinal positions of P_{cr1}, P_{cr2} to P_{cr5}. It could be seen that the lateral positions of these critical points are not always on the same line in the longitudinal direction, with the maximum lateral distance of 2.88mm. N_f is also shown in Figure 10b that the P_{cr2} has the minimum number of cycle to crack initiation. Compared with P_{cr2}, P_{cr1} which is before P_{cr2} and the other three points which are away from nose point have longer fatigue life. Therefore, it is concluded that the fatigue life of the whole crossing is determined by critical point at P=502mm from the nose point.

6. Discussion

6.1 Prediction of crack angles

The predicted angle to the longitudinal direction is 85° to 95°, while the angle to the vertical direction cannot be predicted in this case. In [25] the crack angles of a heavy haul railway based on critical plane approach are calculated. The calculated projection line of the critical plane takes an orientation about 105°-140° to the lateral direction of the rail and an angle of 20° -50° to the longitudinal direction. However it is difficult to validate the crack plane, even if in the field crack initiation is related to many factors, such as loading conditions, friction coefficient as well as material inclusions. In this paper, traction or braking force is not applied to the wheelset, and no variation of friction coefficient is included. Therefore, the crack angles calculated in this paper only give an indication of how the cracks may initiate in the crossing as a reference case.

6.2 Prediction of fatigue life

In [17] the head check initiation life was calculated, which was 9.61×10^4 to 1.23×10^5. The actual crack initiation life (head check) of a normal track was also obtained by field survey. The number of fatigue life cycles was between 5.1×10^4 and 6.07×10^5. Although in this paper the minimum predicted life cycles of 2.1×10^4 are not included in this range, it can be explained by the particular case of turnout crossing where more severe loading conditions and contact conditions are founded.

However, if the material displays ratchetting behaviour (see Figure 2), a criteria proposed in [26] to calculate the number of cycles to crack initiation should be used, which is given by

$$N_r = \frac{\varepsilon_c}{\Delta\varepsilon_r}, \Delta\varepsilon_r = \sqrt{(\Delta\tilde{\varepsilon})^2 + (\Delta\tilde{\gamma}/\sqrt{3})^2} \quad (5)$$

Where ε_c is the critical strain for failure by ratcheting; $\Delta\tilde{\varepsilon}$ and $\Delta\tilde{\gamma}$ are the average ratchetting normal and shear strain per cycle. It was stated that ratchetting and low cycle fatigue (LCF) can be treated as independent and competitive modes for fatigue crack initiation [15]. The number of cycles to crack initiation of the crossing will be calculated separately and compared to determine the dominant fatigue mechanism. However in this paper only one cycle is considered, which is not capable for prediction of ratchetting behaviour.

7. Conclusion

In this paper, a numerical procedure is developed to predict the rolling contact fatigue crack initiation in the crossing. The dynamic responses of the crossing such as stress and strain results are obtained from the FE simulation. Jiang and Sehitoglu fatigue model are then employed for prediction of fatigue life N_f. The results are summarized as follows:

1) Since the crossing geometry varies, contact conditions such as contact angle, contact

point and the contact radius are also changing. Therefore, stress/strain analysis as well as fatigue analysis of the crossing should be considered according to different positions.

2) The critical position on the crossing is around 502mm to the nose point. The maximum Von Mises stress of this position occurs on the surface. Several subsurface points are also selected for fatigue life analysis, which shows that the minimum N_f is determined by the surface critical point.
3) The angles of crack plane can be determined by the angle to the longitudinal direction and vertical direction. It is concluded that according to the simulation, angle to the longitudinal direction of the selected points is 85° to 100°, while the angle to the vertical direction cannot be predicted because of the large variation of the selected points.
4) Five contact positions (P_{cr1} to P_{cr5}) are selected along the crossing for calculation of critical plane angle and N_f. It gives the similar conclusion as 3) that the angle between this plane to longitudinal direction has a possible angle of 85° to 95°, while the angle between this plane to vertical direction is difficult to predict.
5) P_{cr} has the minimum number of cycle to crack initiation, which determines the minimum cycles to crack initiation. Therefore, for rolling contact fatigue problem the weakest position of the crossing is always the position of impact. High impact force leads to high stress and plastic strain, which ultimately determine the minimum fatigue life of the crossing.

Reference

1 Tribology of the Wheel-Rail Contact, Handbook of Railway Vehicle Dynamics, ISBN-13:978-0-8493-3321-7.

2 V.L.Markine, Combatting RCF on switch points by tuning elastic track properties, Wear, 271 (2011), 158-167.

3 M. Wiest, W.Daves, F.D.Fisher, H.Ossberger, Plastification and damage in wheel-rail rolling contact-case study on a crossing. Proc. Appl. Math. Mech. 5, 2005, 67-70.

4 M. Wiest, W.Daves, F.D.Fisher, H.Ossberger, Deformation and damage of a crossing nose due to wheel passages, Wear, 265(2008), 1431-1438.

5 B.A.Palsson, Optimisation of Railway Switches and Crossings. PhD thesis. ISBN 978-91-7385-978-3.

6 B.A.Palsson, J.Nielsen, Wheel-rail interaction and damage in switches and crossings, Vehicle System Dynamics, 50 (2012), 43-48.

7 A. Johansson, B.Palsson, M.Ekh, J.Nielsen, M.Ander, J.Brouzoulis, E.Kassa, Simulation of wheel–rail contact and damage in switches & crossings, Wear, 271 (2011),472-481.

8 M. Pletz, M. Daves, W. Yao, H. Ossberger, Rolling Contact Fatigue of three crossing nose materials-multi-scale FE approach, Wear, 314 (2014), 69-77.

9 D. Kujawski, A deviatoric version of the SWT parameter, International Journal of Fatigue, 67, 95-102, 2014.

10 T. Itoh, M. Sakane, M. Ohnami, D. F. Socie, Non-proportional low cycle fatigue criterion for type 304 stainless steel. J. Eng. Mater. Technol. 117,285–292, 1995.

11 J. Li, J. Liu, Q. Sun, Z. –P. Zhang, Y.-J. Qiao, A modification pf Smith-Watson-Topper damage parameter for fatigue life prediction under non-proportional loading, Fatigue & Fracture of Engineering Materials & Structures, 35, 301-316, 2011.

12 Y. Jiang, H. Sehitoglu, A model for rolling contact failure, Wear, 224(1999), 38-49.

13 Y. Jiang, A fatigue criterion for general multiaxial loading, Fatigue & Fracture of Engineering Materials & Structures, 23, 19–32, 2000.

14 S. Wang, Y. Zhou, Y. Xu, H. Li, Rail fatigue crack initiation life prediction under wheelset creep condition, Journal of Tongji University (Natural Science),42 (6),2014.

15 J. Ringsberg, Life prediction of rolling contact fatigue crack initiation, International Journal of Fatigue, 23, 575-586, 2001.

16 O. Onal, D. Canadinc, H. Sehitoglu, K. Verzal, Y. Jiang, Investigation of rolling contact crack initiation in bainitic and pearlitic, Fatigue & fracture of engineering materials & structures, 35, 985-997,2012.

17 M. Makama, H. Matsuda, H. Doi, M. Tsujie, Fatigue crack initiation life prediction of rails using theory of critical distance and critical plane approach, Journal of Computational Science and Technology, 2, 54-69, 2012.

18 R. Lewis, U. Olofsson, Wheel-Rail Interface Handbook, ISBN: 978-1-84569-412-8.

[19] LS-DYNA keyword user' s manual, Volume II, Material Models, May 19,2014.

[20] J. W. Ringsberg, H. Bjarnehed, A. Johansson, B. L. Josefson, Rolling contact fatigue of rails-finite element modelling of residual stresses, strains and crack initiation. Journal of Rail and Rapid Transit, 214,7-19,2000.

[21] L. Xin, V.L. Markine, I.Y. Shevtsov, "Dynamic interaction between the wheel and crossing nose", The Fourteenth International Conference on Civil, Structural and Environmental Engineering Computing (Civil-Comp Press, Cagliari, Italy, 2013).

[22] L. Xin, V.L.Markine, I.Y. Shevtsov, Numerical analysis of the dynamic interaction between wheelset and turnout crossing using explicit finite element method, submitted to Vehicle System Dynamics.

[23] V. L. Markine and I. Y. Shevtsov, "Experimental Analysis of the Dynamic Behaviour of Railway Turnouts," in The Eleventh International Conference on Computational Structures Technology, Dubrobnik, Croatia, 2012

[24] M. Wiest, E. Kassa, W. Daves, J.C.O. Nielsen, H. Ossberger, Assessment of methods for calculating contact pressure in wheel-rail/switch contact, Wear, 265,1439-1445,2008.

[25] S. Wang, Y. Zhou, Y. Xu, H. Li, Angles and location of a RCF crack in heavy haul railways based on the critical plane, Proceedings of the Second International Conference on Railway Technology: Research, Development and Maintenance, J. Pombo, Civil-Comp Press, Stirlingshire, Scotland, 2014.

[26] A. Kapoor, A re-evaluation of the life to rupture of ductile metals by cyclic plastic strain, Fatigue & Fracture of Engineering Materials & Structures, 17 (2), 38-49, 1994.